Targeting megakaryocytic induced fibrosis by AURKA inhibition in the myeloproliferative neoplasms

The Harvard community has made this article openly available. Please share how this access benefits you. Your story matters

Citation	Wen, Q. J., Q. Yang, B. Goldenson, S. Malinge, T. Lasho, R. K. Schneider, L. J. Breyfogle, et al. 2015. "Targeting megakaryocytic induced fibrosis by AURKA inhibition in the myeloproliferative neoplasms." Nature medicine 21 (12): 1473-1480. doi:10.1038/nm.3995. http://dx.doi.org/10.1038/nm.3995.
Published Version	doi:10.1038/nm.3995
Citable link	http://nrs.harvard.edu/urn-3:HUL.InstRepos:27320308
Terms of Use	This article was downloaded from Harvard University's DASH repository, and is made available under the terms and conditions applicable to Other Posted Material, as set forth at http://nrs.harvard.edu/urn-3:HUL.InstRepos:dash.current.terms-of-use#LAA

Targeting megakaryocytic induced fibrosis by AURKA inhibition in the myeloproliferative neoplasms

Qiang Jeremy Wen[1,*], **Qiong Yang**[1,*], **Benjamin Goldenson**[1], **Sébastien Malinge**[2], **Terra Lasho**[3], **Rebekka K. Schneider**[4], **Lawrence J. Breyfogle**[4], **Rachael Schultz**[1], **Laure Gilles**[1], **Priya Koppikar**[5], **Omar Abdel-Wahab**[5], **Animesh Pardanani**[3], **Brady Stein**[1], **Sandeep Gurbuxani**[6], **Ann Mullally**[4], **Ross Levine**[5], **Ayalew Tefferi**[3], and **John D. Crispino**[1,#]

[1]Department of Medicine, Division of Hematology and Oncology, Northwestern University, Chicago, IL

[2]Institut Gustave Roussy, Paris, France

[3]Division of Hematology, Mayo Clinic, Rochester, MN

[4]Division of Hematology, Department of Medicine, Brigham and Women's Hospital, Harvard Medical School, Boston, MA

[5]Human Oncology and Pathogenesis Program, Memorial Sloan Kettering Cancer Center, New York, NY

[6]Section of Hematopathology, University of Chicago, Chicago, IL

Abstract

Primary myelofibrosis (PMF) is characterized by bone marrow fibrosis, myeloproliferation, extramedullary hematopoiesis, splenomegaly and leukemic progression. Moreover, the bone marrow and spleen of patients are full of atypical megakaryocytes that are postulated to contribute to fibrosis through the release of cytokines including TGF-β. Although the JAK inhibitor ruxolitinib provides symptomatic relief, it does not reduce the mutant allele burden or significantly reverse fibrosis. Here we show through pharmacologic and genetic studies that, apart from JAK2, Aurora kinase A (AURKA) is a novel therapeutic target in PMF. MLN8237, a selective AURKA inhibitor promoted polyploidization and differentiation of PMF megakaryocytes and displayed potent anti-fibrotic and anti-tumor activity in vivo. We also reveal that loss of one allele of AURKA is sufficient to ameliorate fibrosis and other PMF phenotypes in vivo. Our data suggest that megakaryocytes are drivers of fibrosis and that targeting them with AURKA inhibitors will provide therapeutic benefit in PMF.

#Corresponding author: John D. Crispino, ; Email: j-crispino@northwestern.edu
*These authors contributed equally to this work.

Although the median survival for PMF patients is 5–7 years, those with intermediate and high-risk disease, as defined by the Dynamic International Prognostic Scoring System Plus, have a median survival of just 16–35 months[1]. Patients frequently die from transformation to acute leukemia, pancytopenia, thrombosis and cardiac complications, infections and bleeding[2]. Within the bone marrow, there are excessive megakaryocytes with an abnormal nuclear/cytoplasmic ratio and reduced polyploidy state. In vitro cultures of CD34$^+$ cells have shown that megakaryocytes expand excessively, are immature, and show delayed apoptosis by virtue of increased bcl-xL expression[3]. Mutations associated with PMF include those that affect JAK/STAT signaling (*JAK2, MPL*), ER stress (*CALR*), epigenetic regulators (*TET2* and *ASXL1*) and RNA splicing (*SRSF2, SF3B1*)[4–8]. Although ruxolitinib, a JAK inhibitor approved for use in PMF[9,10], provides symptomatic relief and extends survival, it does not reduce the mutant allele burden or alter the natural history of the disease[2,11,12]. Moreover, many patients are intolerant to, or discontinue therapy due to side effects, including profound anemia and thrombocytopenia[13]. Thus, additional agents that provide sustained therapy, reduce fibrosis and decrease the allele burden are needed.

Several lines of evidence suggest that increased numbers of megakaryocytes contributes to bone marrow fibrosis. First, mice that overexpress thrombopoietin (THPO) develop fibrosis that is associated with an increased megakaryocyte mass[14]. Second, mice with a megakaryocyte deficiency of *Gata1* show elevated numbers of immature megakaryocytes and severe bone marrow fibrosis[15,16]. Third, megakaryocytes from PMF patients secrete increased levels of the fibrotic cytokine TGF-β[3]. However, the extent to which megakaryocytes are required for myelofibrosis and whether targeting the megakaryocyte lineage is sufficient to prevent disease has not been shown.

We recently reported the identification of small molecules that induce megakaryocyte polyploidization, differentiation, and subsequent apoptosis[17]. One of these compounds is the AURKA inhibitor MLN8237[18]. Given that megakaryocytes in PMF show impaired differentiation, we predicted that AURKA inhibition would induce maturation, reduce the burden of immature megakaryocytes and ameliorate the characteristics of PMF, including bone marrow fibrosis. Here, we show that AURKA activity is strongly elevated in cells that harbor activating mutations in *JAK2*, *MPL* and *CALR*. This upregulation is associated with an increase in c-MYC expression downstream of activated JAK/STAT signaling. Furthermore, we demonstrate that MLN8237 induced differentiation and polyploidization of primary PMF megakaryocytes. MLN8237 reduced the disease burden, peripheral blood counts, and the degree of fibrosis of both *Jak2^{V617F}* and MPLW515L mice. Finally, we reveal that AURKA is a *bona fide* target in PMF, as loss of a single allele is sufficient to prevent myelofibrosis and other PMF phenotypes in vivo. Together our work shows that megakaryocytes are required for development of PMF and targeting these cells is a novel therapeutic strategy.

Results

Inhibition of AURKA induces differentiation of JAK2 and MPL mutant cells

Based on our previous studies, which showed that the AURKA inhibitor MLN8237 promotes maturation of malignant megakaryocytes, and our hypothesis that atypical megakaryocytes directly contribute to myelofibrosis, we investigated the activity of AURKA inhibitors in PMF. First, we assayed the effect of MLN8237 on the human erythroleukemia (HEL) cell line because it is JAK2V617F[+] and is responsive to JAK2 inhibition[19]. MLN8237 caused decreased phosphorylation of AURKA, but not STAT3 or STAT5, whereas ruxolitinib inhibited phosphorylation of STAT3 and STAT5, but not AURKA (Supplementary Fig 1a). MLN8237 potently inhibited cell growth with an IC50 of 26.5nM, whereas the IC50 for ruxolitinib was 343nM (Supplementary Fig 1b). MLN8237 induced polyploidization and upregulation of the megakaryocyte cell surface markers CD41 and CD42 (Supplementary Fig 1c – e). In contrast, ruxolitinib did not have these differentiation effects. Similarly, MLN8237, but not ruxolitinib, displayed growth inhibition and megakaryocyte differentiation activity on the G1ME/MPLW515L cell line (Supplementary Fig 2), which lacks the erythromegakaryocytic transcription factor GATA1 and expresses the activated allele of MPL. This cell line, derived from *Gata1*-deficient embryonic stem cells, can differentiate into megakaryocytes upon restoration of GATA1[20]. G1ME cells are relevant to PMF because patients express reduced levels of GATA1[21] and mice that lack GATA1 in megakaryocytes develop profound bone marrow fibrosis[16]. Finally, similar effects were observed in SET-2 cells, a human megakaryocytic cell line derived from a patient with JAK2V617F[22]. (Supplementary Fig 3 a – e).

Next, we extracted protein from bone marrow cells of *Jak2*[V617F] knock-in mice[23] or mice transplanted with mouse bone marrow cells overexpressing MPLW515L or two different calreticulin mutants (CALR type 1 and CALR type 2)[24,25] and then assayed phosphorylation of AURKA, STAT3, and STAT5. As expected, JAK2V617F, MPLW515L, and CALR mutants induced phosphorylation of STAT5 relative to controls (Fig 1a and Supplementary Fig 4). Moreover, expression of these mutants led to a striking upregulation of AURKA. MLN8237 led to a decrease in AURKA phosphorylation without affecting the levels of p-STAT3 or p-STAT5 after 6 hours of culture (Fig 1b,c). Of note, treatment of these cells with increasing doses of ruxolitinib caused a decrease in p-STAT3 and p-STAT5, but did not reduce the level of p-AURKA until 24 hours and only at doses above 1μM (Supplementary Fig 5). Together, these results show that AURKA is upregulated by JAK2V617F, MPLW515L and CALR mutants, and that MLN8237 and ruxolitinib differentially affect cell signaling. To confirm that p-Aurka is indeed elevated in megakaryocytes, we cultured MPLW515L expressing bone marrow cells with THPO. As we previously reported[26], the expression of AURKA declines with megakaryocyte maturation, such that very little protein is detected in control cells following three days of culture (Supplementary Fig 6). In contrast, megakaryocytes that express MPLW515L displayed persistent p-AURKA through 7 days of culture.

We next assessed the effect of AURKA inhibition on the growth of MPLW515L bone marrow cells. MLN8237 significantly increased the expression of CD41 and CD42, the

degree of polyploidization, and annexin V staining of megakaryocytes (Fig 1d – g). These results are consistent with our previous observations that inhibition of AURKA promotes megakaryocyte differentiation and acts to suppress proliferation of the lineage. Finally, we transduced mouse bone marrow cells with retroviruses that harbor WT or MPLW515L and cultured the cells in methylcellulose in the presence of increasing doses of MLN8237. MLN8237 preferentially inhibited colony forming unit megakaryocyte (CFU-MK) and colony-forming unit myeloid (CFU-Myeloid) of the MPLW515L expressing cells relative to MPLWT expressing cells even at doses as high as 1μM (Fig 1h – i). This selective effect is likely due to a greater dependence of the cells with activated JAK/STAT signaling on AURKA activity.

Previous studies have reported that AURKA expression is elevated downstream of JAK2V617F and that effect this is mediated by increased c-MYC[27–29]. Consistent with this model, we observed increased c-MYC protein in bone marrow cells expressing either Jak2V617F or MPLW515L (Fig 1a). To investigate the link between activated JAK/STAT signaling, MYC and AURKA, we returned to SET-2 cells. c-MYC is readily detected in SET-2 extracts and its expression is significantly reduced by ruxolitinib at 48 hours (Supplementary Fig 3f,g). This reduction coincided with a decrease in both total and p-AURKA. In contrast, MLN8237 did not affect c-MYC, indicating that the inhibitor is working downstream of the JAK/STAT-MYC axis. To confirm that c-MYC is required for elevated AURKA expression, we knocked down c-MYC with two shRNAs. As predicted, we detected reduced levels of total and pAURKA (Supplementary Fig 7a). This reduction of AURKA was associated with increased expression of CD41 and CD42 and apoptosis (Supplementary Fig 7b – e). Of note, the increase in PI3K/AKT signaling that is observed in *JAK2* and *MPL* mutant cells (Fig 1a) is not responsible for the increase in p-AURKA, as the AKT inhibitor MK-2206 did not change the level of p-AURKA (Supplementary Fig 8).

We next investigated whether AURKA is upregulated in MPN patients (Supplementary Tables 1,2). Western blot analysis revealed that p-AURKA and AURKA are elevated in CD34+ cells of PMF patients and in mononuclear cells of individuals with ET or PV (Fig 2a, Supplementary Fig 9,Supplementary Fig 10). We also observed elevated expression of c-MYC, as predicted by studies with mouse cells and the SET-2 cell line. Similar to what we observed in these two aforementioned settings, treatment of primary PMF CD34+ cells with MLN8237 led to suppression of p-AURKA, but not of JAK/STAT signaling (Fig 2b,c). Furthermore, while ruxolitinib treatment rapidly reduced p-STAT5, it did not affect p-AURKA until prolonged incubation. Together these results support the model that enhanced JAK/STAT signaling indirectly leads to an increase in p-AURKA.

We next investigated the effects on MLN8237 on CD34+ cells collected from the peripheral blood of patients with PMF (PMF 5–14, Supplementary Table 1). MLN8237 significantly induced up-regulation of CD41 and CD42 (Fig 2d,e) and induced polyploidization of CD41+ cells without affecting the DNA content of CD41− cells (Fig 2f). Finally, consistent with MLN8237 acting as a suppressor of the megakaryocyte lineage, it also inhibited cell growth (Fig 2g).

Inhibitors of AURKA provide therapeutic benefit in MPN animal models

Before testing MLN8237 in MPN models, we treated healthy Balb/C mice with 15mg/kg bid for three weeks. Pharmacokinetic studies revealed that a single dose of 15mg/kg exceeds the IC50 for growth inhibition in primary bone marrow MPLW515L expressing cells for >12 hours in mice[17]. MLN8237 was well tolerated, with no reductions in body weight, peripheral blood counts, or bone marrow composition (Supplementary Fig 11). Histological analysis confirmed that MLN8237 did not cause myelosuppression or any other detrimental effects when used at this dose..

Transplantation of bone marrow cells expressing MPLW515L leads to an aggressive MPN characterized by marked leukocytosis, thrombocytosis, hepatomegaly, splenomegaly and the presence of abnormal megakaryocytes that is accompanied by bone marrow fibrosis in recipient animals[30,31]. We transplanted bone marrow harboring MPLW515L to irradiated Balb/C recipient mice, waited three weeks, and verified that all animals had >50% GFP in the peripheral blood (Q.W., data not shown). After randomizing the mice, we then treated them with 15mg/kg MLN8237, 60mg/kg dimethylfasudil (diMF)[17] or vehicle twice daily for three weeks. As expected, vehicle treated mice developed an aggressive PMF syndrome that worsened with time[30,31] (Fig 3). In contrast, both AURKA inhibitors normalized the white cell and platelet counts and also reduced the hematocrit and hemoglobin, the latter of which are only modestly elevated in this model (Fig 3a,b and Supplementary Fig S12a). MLN8237 and diMF reduced the spleen and liver weights without affecting the body weight (Fig 3c and Q.W. data not shown). Both drugs also reduced the GFP$^+$ tumor cell population as well as the degree of MPLW515L expression as measured by significant decreases in the median fluorescence intensities in the spleen (Fig 3d). Consistent with MLN8237 and diMF acting as suppressors of the megakaryocyte lineage, we observed vast reductions in the CD41 and CD42 populations in the spleen as well as an increased degree of megakaryocyte polyploidization (Fig 3e – g). MLN8237 and diMF had similar effects on bone marrow megakaryocytes (Supplementary Fig S12b,c). Both drugs also reduced the splenic Gr1$^+$/Mac1$^+$ populations and the LSK and myeloid progenitor populations in the bone marrow (Supplementary Fig 12d,e and Q.W. data not shown). Importantly, consistent with a previous report that PMF megakaryocytes secrete excessive TGF-β[3], we observed significant reductions in TGF-β in the plasma of animals following MLN8237 or diMF treatment (Fig 3h). Bone marrow histology revealed a robust drop in megakaryocyte mass that was accompanied by a striking decline in fibrosis in animals treated with either MLN8237 or diMF (Fig 3i,j). We also observed decreased tumor burden in the peripheral blood, spleen, lung and liver (Supplementary Fig 12f – j), as well as decreased fibrosis in the spleen (Supplementary Fig 12j). Finally, we repeated this study in mice with a more fulminant disease, by waiting 30 days after transplant. In this setting MLN8237 rapidly normalized the peripheral blood counts, and decreased splenomegaly, hepatomegaly, and the megakaryocyte burden (Supplementary Fig 13a – e). This was accompanied by normalization of peripheral blood cytomorphology and bone marrow, spleen, lung and liver histology along with variable reduction in bone marrow fibrosis (Supplementary Fig S13f – j and Q.W. data not shown).

We next studied the activity of MLN8237 in $Jak2^{V617F}$ knockin mice[23]. Following activation of V617F allele, these animals develop polycythemia, mild leukocytosis, perturbed megakaryopoiesis, splenomegaly, hepatomegaly and myelofibrosis. We transplanted recipient mice with bone marrow cells from the knockin mice with Vav-Cre mediated expression of JAK2V617F and observed polycythemia, leukocytosis, and thrombocytosis in the recipients four weeks after transplantation. We then treated the animals with 15mg/kg MLN8237 by oral gavage twice daily for seven weeks. MLN8237 significantly reduced the WBC, hematocrit, platelet counts, and spleen weight without affecting the body weight (Fig 4a,b and Q.W. data not shown). Within the bone marrow and spleen, MLN8237 reduced the number of erythroid cells and megakaryocytes and induced megakaryocyte polyploidy (Fig 4c – g). Moreover, MLN8237 normalized bone marrow megakaryopoiesis and splenic architecture (Fig 4h,i). MLN8237 also strikingly attenuated fibrosis in the bone marrow (Fig 4j).

Aurka is required for myelofibrosis

Complete loss of *Aurka* results in early embryonic lethality due to impaired centrosome separation and defects in bipolar spindle formation, while mice with heterozygous deficiency are viable, fertile and show no hematopoietic defects[32]. In order to determine the requirement for AURKA expression in development of myelofibrosis, we crossed *Aurka* floxed mice with MX1-Cre mice. Bone marrow cells from $Aurka^{F/+}$ and $Aurka^{F/+}$ MX1-Cre mice were transduced with MPLW515L and transplanted to lethally irradiated recipients. We observed equivalent levels of engraftment as measured by GFP at 3 weeks post-transplant (Fig 5a). At this time point, we injected $Aurka^{F/+}$ MX1-Cre and $Aurka^{F/+}$ mice with polyinosinic/polycytidylic acid (pIpC), which resulted in complete excision of the single allele of *Aurka* in the peripheral blood, bone marrow, and spleen (Fig 5b). Shortly after pI-pC injection, we observed progression of leukocytosis and thrombocytosis in the control group, but not in the heterozygous deleted group (Fig 5c,d). In contrast to the expansion in the GFP$^+$ tumor population in the control group, the $Aurka^{F/+}$ MX1-Cre excised tumor cells failed to expand after excision (Fig 5a). The loss of only one allele of *Aurka* also led to significant reductions in the spleen and liver weights and decreased GFP positive cells with reduced median fluorescence intensities in the spleen (Fig 5e,f and Supplementary Fig 14a). In addition, heterozygous loss of *Aurka* led to decreased CD41$^+$ and Gr1$^+$/Mac1$^+$ cells in the spleen, but an increase in the degree of megakaryocyte polyploidization (Fig 5g,h and Supplementary Fig 14b). Finally, the deletion decreased the tumor burden in the peripheral blood, bone marrow, spleen, lung and liver, and the degree of bone marrow fibrosis (Fig 5i,j and Supplementary Fig 14c – f). As expected based on our data that mice with complete loss of Aurka develop rapid bone marrow failure[26], loss of both alleles of *Aurka* also led to resolution of the disease while nearly eliminating the GFP+ tumor cell population (Supplementary Fig 15). Together these results show that the full dosage of *Aurka* is required for the initiation and/or progression of MPN in the MPLW515L model and reveal that AURKA is indeed a valid target for therapy.

MLN8237 synergizes with ruxolitinib in vitro and in vivo

In order to determine whether AURKA inhibitors can increase the effectiveness of ruxolitinib, we analyzed the ability of these agents to synergize with one another. Given that

MLN8237 targets the AURKA pathway and that ruxolitinib has a primary effect on the STAT pathway, we predicted that the compounds would synergize with one another. First, we determined the IC50s of MLN8237 and ruxolitinib on CFU-myeloid formation by cells harvested from MPLW515L bone marrow recipient mice. We found that MLN8237 and ruxolitinib displayed similar effects, with IC50s of 19.4nM and 22.7nM respectively (Fig 6a). Next, we analyzed the effect of different doses of MLN8237 and ruxolitinib and found that the combinations inhibited colony formation to a much greater degree than either single agent, and that this combination showed synergy at multiple doses (Supplementary Table 3).

Next, we evaluated the activity of the combination in vivo. Wild-type bone marrow cells expressing MPLW515L were transplanted to irradiated recipients. Three weeks following engraftment, we treated animals with sub-maximal doses of MLN8237 or ruxolitinib as single agents or in combination. Whereas the single agents at these doses did not alter disease progression, the combination of the drugs led to marked reductions in both the white cell and platelet counts (Fig 6b,c) and significant decreases in the megakaryocyte burden within the bone marrow and spleen (Fig 6d,e). The efficacy of the combination was further confirmed by major reductions in the tumor burden in the peripheral blood, bone marrow, spleen, lung and liver (Fig 6f – h and Q.W. data not shown). Finally, the combination of MLN8237 and ruxolitinib effectively eliminated bone marrow fibrosis (Fig 6i). Together these results demonstrate that MLN8237 synergizes with ruxolitinib and suggest that a combination of each agent will show superior activity in patients.

Discussion

In 1984, Castro-Malaspina proposed that ineffective megakaryopoiesis and accumulation of intracytoplasmic components led to an increase in a megakaryocyte growth factor (later shown to be PDGF) and a decrease in PF4 within the bone marrow[33]. This combination of elevated PDGF, which increased collagen production, and reduced PF4, which decreased collagen degradation, would then lead to a net increase in collagen and fibrosis. Subsequent studies have shown elevated PDGF, TGF-β, and bFGF in megakaryocytes and platelets of PMF patients[3,34,35]. More recently, BMPs and oncostatin M have been implicated in myelofibrosis[36,37]. Of these, TGF-β produced by megakaryocytes likely plays a critical role, as this cytokine is required for fibrosis that results from increased THPO expression[38].

Whether immature megakaryocytes also drive the other phenotypes in PMF has been less clear. While the recipients of THPO expressing bone marrow progenitors developed a lethal myeloproliferative disorder with fibrosis and other PMF phenotypes, expression of the transgene was not restricted to megakaryocytes[14]. Moreover, the *Gata1*low strain, which primarily has defects in megakaryocytes, develops fibrosis with secondary erythroid defects, but not leukocytosis[16]. These observations suggest that multiple hematopoietic lineages are necessary for PMF. Of note, two elegant recent studies using the PF4-Cre strain have shown that megakaryocytes influence HSC quiescence[39,40], suggesting that malignant megakaryocytes may have a direct adverse effect on the HSC population. These observations also lend credence to the model that aberrant megakaryocytes drive the entire spectrum of PMF phenotypes. This conclusion does not preclude contributions to fibrosis from other cells, such as osteoblastic lineage cells (OBCs), which can be remodeled into inflammatory

myelofibrotic cells by exposure to BCR-ABL expressing bone marrow cells[41]. Although this latter study implicated Mac1^{+} myeloid cells in the conversion of OBCs, the authors did not examine the role of megakaryocytes in the process.

In general, AURKA is highly expressed in tumor cells, making it a potential cancer therapeutic. Indeed, we find that the levels of total and phosphorylated AURKA are greatly elevated in cells that express mutant CALR, MPLW515L or JAK2V617F. Although we cannot formally exclude the possibility that AURKA levels are higher in PMF megakaryocytes in part because they are less mature, the observation that AURKA is also elevated in peripheral blood mononuclear cells and purified CD34^{+} cells indicates that high levels of AURKA is a common feature of hematopoietic cells in PMF. Mechanistically, we provide evidence that this phenomenon is mediated by increased expression of c-MYC, which has been shown to be a downstream consequence of activated JAK2[27–29]. The subsequent increase in the level of p-AURKA is likely the result of autophosphorylation[42].

Finally, we discovered that AURKA levels are critically important for the MPNs, as loss of a single allele led to profound decrease in tumor burden in vivo without affecting engraftment or inducing myelosuppression. This latter observation, combined with the observed tolerance and lack of myelosuppression at the effective doses of MLN8237 in our animal models, suggests that there is a therapeutic window for which the inhibitor will be effective against the disease without disrupting normal hematopoiesis.

Online Methods

Compounds and plasmids

MLN8237 and diMF were prepared and characterized by ^{1}H NMR (and optical rotation for diMF) by the Broad Institute as previously reported[17]. Ruxolitinib was purchased from EMD Chemicals. MK-2206 was purchased from Selleck Chemicals. Migr1-GFP-MPLW515L, Migr1-GFP-JAK2V617F, Migr1-GFP-CALR T1, and Migr1-GFP-CALR T2 were created by subcloning and were validated by sequencing. Glycerol stocks of empty pLKO.1 or the pLKO.1 c-Myc shRNAs (TRCN0000039640 (sh40) and TRCN0000039642 (sh42) were purchased from Sigma-Aldrich.

Cell Culture

Human HEL cells (obtained from ATCC) were grown in RPMI Media 1640 supplemented with 10% FBS and antibiotics (100 mg/ml penicillin/streptomycin mix). Human SET-2 cells (obtained from Dr. T. Arima)[22] were grown in RPMI Media 1640 supplemented with 20% FBS and antibiotics (100 mg/ml penicillin/streptomycin mix). G1ME cells (obtained from Dr. Mitchell Weiss) were grown in α-MEM media supplemented with 20% FBS and 1% THPO conditioned medium as described previously[20]. For mouse primary bone marrow cell cultures, progenitor cells were enriched from bone marrow of untreated mice either by lineage negative (Lin-) selection using a progenitor cell enrichment kit (Stemcell Technologies) or by c-Kit positive selection using a kit from Miltenyi Biotec. Mouse bone marrow progenitor cells were cultured in StemSpan (Stemcell technologies) supplemented with 10ng/mL mouse IL-3, 10ng/mL human IL-6 and 40 ng/mL mouse SCF, along with

human LDL (20 μg/mL). To derive megakaryocytes, lineage-depleted mouse bone marrow cells were cultured in the presence of THPO (20 ng/mL) in RPMI Media 1640 supplemented with 10% FBS and antibiotics (100 mg/ml penicillin/streptomycin mix) for various period of time. Human mononuclear cells were separated from peripheral blood of PMF, ET or PV patients using Ficoll-Paque PLUS (GE HealthCare Life Sciences) according to the manufacturer's instructions. Human CD34+ cells were purified from mononuclear cells of PMF patients using a kit from Miltenyi Biotec. Human CD34$^+$ cells were cultured in serum-free medium in the presence of recombinant 10ng/ml human THPO. Ingredients used to prepare the serum-free medium were previously described[17]. The cultured cells were maintained in a humidified atmosphere at 37 °C with 5% CO_2. Cell lines were tested and determined to be mycoplasma free.

Viral transduction

For the retroviral experiments, plat-E cells (5×10^6) were seeded in a 10-cm dish the day before transfection and then transfected with Migr1 containing human MPLW1515L or human Calreticulin type 1 (CALR T1) or type 2 (CALR T2) mutations using Fugene VI (Roche) following the manufacturer's protocols. Forty-eight hours after transfection, the viral supernatant was collected and 2 ml of viral supernatant was mixed with 5×10^6 of mouse bone marrow progenitor cells or G1ME cells in the presence of 8 μg/ml polybrene and 10mM HEPES, and then centrifuged at 2,500 rpm for 90 min at 32 °C. Spinoculation was performed 2 times on the second day after extraction of bone marrow cells. For the lentiviral experiments, 293T cells (5×10^6) were seeded in a 10-cm dish the day before transfection and then transfected with empty pLKO.1, or two different c-MYC shRNAs with Fugene VI (Roche). Forty-eight hours after transfection, the viral supernatant was collected, two ml of viral supernatant was mixed with 5×10^6 of SET-2 cells in the presence of 8 μg/ml polybrene and 10mM HEPES, and the cells were centrifuged at 2,500 rpm for 90 min at 32°C. Spinoculation was performed twice on the same day.

In vitro inhibitor assays

Cell lines were plated in 12-well tissue culture-treated plates in 2 ml media with DMSO or chemical inhibitors for various period of time. At the end of the incubation, cell viability was assessed using the Trypan blue staining (Sigma) or the CellTiter proliferation assay (Promega). Results were normalized to growth of cells in media containing an equivalent volume of DMSO. The effective concentration at which 50% inhibition in proliferation occurred (IC50) was determined using Graph Pad Prism 5.0 software. Primary mouse bone marrow cells were incubated with DMSO or chemical inhibitors in the presence of 10 ng/mL mouse THPO after retroviral transduction. At the end of the incubation, cell surface markers, DNA content and Annexin V staining were evaluated by flow cytometry.

CFU assays

Assays of colony forming unit megakaryocyte (CFU-MK) and colony forming unit myeloid (CFU-myeloid) cells were performed on mouse lineage negative cells. For CFU-MK assay, 5,000 bone marrow lineage negative cells were seeded in Megacult-C medium (Stemcell Technologies) supplemented with 10ng/ml mouse IL-3, 10 ng/ml human IL-6, and 50 ng/ml of mouse THPO and cultured in the presence of DMSO or chemical inhibitors for 7–9 days.

For CFU-myeloid assay, 2,000 bone marrow lineage negative cells were seeded in MethoCult medium (Stemcell Technologies) supplemented with 10ng/ml mouse IL-3, 10 ng/ml human IL-6, 10 ng/ml mouse SCF and 10 ng/ml of mouse granulocyte-monocyte colony stimulating factor (GM-CSF), and cultured in the presence of DMSO or chemical inhibitors for 7 days. Slides of Megacult cultures were fixed with methanol and then were stained with substrates of acetylcholinesterase according to the manufacturer's instructions. Only stained colonies were counted. For the CFU-myeloid assay, CFU-G, CFU-M and CFU-GM were enumerated on day 7 according to the manufacturer's instructions. The number of CFU-myeloid colonies was taken as the sum of CFU-G, CFU-M and CFU-GM.

Synergy studies

C57BL/6 mouse bone marrow cells were extracted and enriched for c-Kit positive cells. Bone marrow cells were transduced with Migr1 containing human MPLW1515L and transplanted into lethally irradiated animals. Three weeks later, mouse bone marrow cells were harvested and then plated into MethoCult medium (Stemcell Technologies) with cytokines in the presence of DMSO, MLN8237 or ruxolitinib. The myeloid colonies were enumerated 7 days later and expressed as a fraction of samples treated with DMSO. Dose-response curves were generated in Graph Pad Prism software. Combination indices were determined using the median-effect principle of Chou and Talalay (CalcuSyn Software)[43].

Animal experiments

Aurka floxed mice on the C57BL/6 background[32] were obtained from Dr. Terry Van Dyke and were crossed to MX1-Cre mice to generate $Aurka^{F/+}$ MX1-Cre and $Aurka^{F/F}$ MX1-Cre mice. $JAK2^{V617F}$ knock-in mice on the C57BL/6 background have been described previously[23]. For the MPLW515L model, Balb/c bone marrow progenitor cells were enriched by c-Kit positive selection and cultured overnight. The next day, the cells were transduced with human MPLW515L retrovirus. On the third day, recipient Balb/c mice were transplanted with transduced bone marrow cells after being lethally irradiated with two doses of 550 rads within 24 hours and then transplanted with 0.3 million GFP+ cells. Recipient mice developed leukocytosis, polycythemia and thrombocytosis in 2–3 weeks. For JAK2V617F cell transplants, bone marrow cells from $JAK2^{V617F}$ knock-in mice with Vav-Cre mediated expression were extracted and a total of one million cells were transplanted into irradiated recipient animals. In the drug studies, mice were randomized to treatment groups based on the level of GFP+ tumor cells in the peripheral blood. Vehicle, MLN8237 or diMF were fed to transplant recipients of MPLW515L or JAK2V617F cells by oral gavage twice a day, 5 days a week. In these drug studies, the experimental design was blinded in such as way that the researcher assessing the outcome was unaware of the treatment groups. For the genetic study, 3 doses of pI-pC (GE HealthCare) at 20 mg/kg were given to $Aurka^{F/+}$, $Aurka^{F/+}$ MX1Cre, $Aurka^{F/F}$, or $Aurka^{F/F}$ MX1Cre mice on every other day by i.p. injection. All experiments were conducted in accordance with animal protocols approved by the Northwestern University Institutional Animal Care and Use Committee. Group sizes were determined by performing a power calculation to lead to a 90% chance of detecting a significant difference ($p<0.05$) in the megakaryocytic tumor burden across the treatment groups. Female mice between 8 and 12 weeks of age were used for all transplant studies.

Complete blood counts

Blood (50 μL) was collected from the tail vein in EDTA-coated tubes and analyzed by a Hemavet 850 complete blood counter (Oxford, CT).

Flow Cytometry

Bone marrow cells were flushed from hind leg bones with PBS (GIBCO) + 2% FBS + penicillin/streptomycin (Cambrex, Biowhittaker). Spleen cells were prepared by pressing tissue through a cell strainer. In both cases, cells were lysed on ice with red blood cell lysis solution (Puregene). Single-cell suspensions of bone marrow, spleen or cell lines were prepared by resuspending the cells in PBS with 0.5% BSA (Sigma) and 2mM EDTA (Gibco). Surface marker staining for human or mouse CD41 (GPIIb; BD Bioscience 561850 (mouse) and 555469 (human), San Diego, CA) and CD42b (GPIb; BD Bioscience 551061 (human) or Emfret Analytics M040-3 (mouse), Wurzburg, Germany) was performed by incubation for 30 minutes in Ca_2^+ free, Mg_2^+ free phosphate-buffered saline (PBS). Other mouse surface makers, such as Ter119 (BD Bioscience 0560504), CD71 (BD Bioscience 555535), Gr-1 (BD Bioscience 553129), and Mac1 (BD Bioscience 555388) were stained in a similar fashion. Mouse bone marrow cells were also stained with a mouse hematopoietic progenitor enrichment kit (Stemcell Technologies 19756) that contained CD5, CD11b, CD19, CD45R, Gr-1, and TER119, followed by pacific blue-labeled streptavidin. Cells were simultaneously stained with antibodies against c-Kit (eBioscience 17–1171), Sca-1 (eBioscience 25–5981), CD34 (eBioscience 13–0341) and FcγR (eBioscience 45–0161) to label stem and myeloid progenitor populations, including LSK, CMP, GMP and MEP, as previously described[44]. For annexin V staining, cells were incubated with an annexin V antibody (BioVision K103-25) in staining buffer (10 mM HEPES, 140 mM NaCl, 2.5 mM $CaCl_2$, pH 7.4) for 15 min. For DAPI staining, mouse or human cells were fixed in 2% paraformaldehyde at room temperature for 10 minutes and stained with 4, 6-diamidino-2-phenylindole (DAPI; Sigma)/saponin solution containing 0.1% saponin and 1 μg/mL DAPI to determine the DNA content. DNA content, surface marker expression, myeloid progenitor staining and apoptosis were determined using a LSR II flow cytometer (BD Biosciences). Data were analyzed using FlowJo software (Treestar, Ashland, OR). In the experiment with differentiation of mouse lineage-depleted bone marrow cells to megakaryocytes, cells were stained with the anti-CD41 antibody and sorted using a FACSAria instrument (Becton Dickinson, Mountain View, CA).

PCR analysis

Genomic DNA was extracted from mouse BM, spleen and peripheral blood cells using a kit from Qiagen. To detect the *Aurka* WT and floxed alleles, forward (5′-CCTGTGAGTTGGAAAGGGACATGG CTG-3′) and reverse (5′-CCACCACGAAGGCAGTGTTCA ATC CTA AA −3′) primers were used to amplify 500 and 600 bp PCR products, respectively. To detect the excision of *Aurka* floxed allele, forward (5′-CAGAGTCTAAGTCGAGATATCACC TGAGGGTTGA-3′) and reverse (5′-GATGGAAACCCT GAGCACCTGTGA AAC −3′) primers were used to amplify a 300bp PCR product. To detect the MX1 Cre transgene, forward (5′-GCCTGCATTACCGGTCGATGCAACGA-3′) and reverse (5′-

GTGGCAGATGGCGCGGCAACACCAT-3′) primers were used to amplify a 600bp PCR product.

Western blots

Cells were lysed in RIPA buffer (Tris-HCl, 50 mM, pH 7.4; NP-40, 1%; Na-deoxycholate, 0.25%; NaCl, 150 mM; EDTA, 1 mM) supplemented with protease inhibitors (pepstatin, leupeptin, aprotinin, each 10 μg/ml; PMSF, 1 mM) and phosphatase inhibitor (Na_3VO_4, 1 mM). Proteins were separated by SDS-PAGE and transferred to a PVDF membrane. Membranes were blotted with antibodies detecting phospho-AURKA (Cell Signaling 2914), phospho-STAT3 (Cell Signaling 9145), phospho-STAT5 (Cell Signaling 9359), STAT3 (Cell Signaling 4904), STAT5 (Cell Signaling 9363), AURKA (GeneTex GTX13824), GRB2 (BD Bioscience 610111) and HSC70 (Santa Cruz Biotechnology SC7298).

Histopathology

Tissues were fixed in 10% neutral buffered formalin, embedded in paraffin, and stained with hematoxylin and eosin or with reticulin to assess for fibrosis. Blood smears were fixed in methanol and stained in Giemsa and May-Grunwald solutions.

Images of histological slides were obtained on a Leica DM4000B microscope (Leica) equipped with a Leica DFC320 color digital camera (Leica).

Patient Samples

Primary specimens from patients with PMF, ET or PV were obtained after informed consent in accordance with protocols approved by the Northwestern University and the Mayo Clinic Institutional Review Boards. Details on each patient are provided in Supplementary Tables 1 and 2.

Statistics

For quantitative assays, treatment groups were reported as mean ± SD and compared using the unpaired two-sided Student's t test. When multiple comparisons were necessary, one-way or two-way analysis of variance with post-test Bonferroni correction was used. Statistical significance was established at p less than or equal to 0.05, labeled as *, p 0.05 and **, p 0.01. All analysis was performed using GraphPad Prism Version 4.01 for Windows (GraphPad Software).

Supplementary Material

Refer to Web version on PubMed Central for supplementary material.

Acknowledgments

References

1. Gangat N, et al. DIPSS plus: a refined Dynamic International Prognostic Scoring System for primary myelofibrosis that incorporates prognostic information from karyotype, platelet count, and transfusion status. Journal of Clinical Oncology. 2011; 29:392–397. [PubMed: 21149668]

2. Mascarenhas J, Hoffman R. A comprehensive review and analysis of the effect of ruxolitinib therapy on the survival of patients with myelofibrosis. Blood. 2013; 121:4832–4837. [PubMed: 23570800]

3. Ciurea SO, et al. Pivotal contributions of megakaryocytes to the biology of idiopathic myelofibrosis. Blood. 2007; 110:986–993. [PubMed: 17473062]

4. Vannucchi AM, et al. Mutations and prognosis in primary myelofibrosis. Leukemia. 2013; 27:1861–1869. [PubMed: 23619563]

5. Abdel-Wahab O, et al. Unraveling the genetic underpinnings of myeloproliferative neoplasms and understanding their effect on disease course and response to therapy: proceedings from the 6th International Post-ASH Symposium. American Journal of Hematology. 2012; 87:562–568. [PubMed: 22460584]

6. Tibes R, Bogenberger JM, Benson KL, Mesa RA. Current outlook on molecular pathogenesis and treatment of myeloproliferative neoplasms. Molecular Diagnosis & Therapy. 2012; 16:269–283. [PubMed: 23023734]

7. Klampfl T, et al. Somatic mutations of calreticulin in myeloproliferative neoplasms. New England Journal of Medicine. 2013; 369:2379–2390. [PubMed: 24325356]

8. Nangalia J, et al. Somatic CALR mutations in myeloproliferative neoplasms with nonmutated JAK2. New England Journal of Medicine. 2013; 369:2391–2405. [PubMed: 24325359]

9. Verstovsek S, et al. A double-blind, placebo-controlled trial of ruxolitinib for myelofibrosis. N Engl J Med. 2012; 366:799–807. [PubMed: 22375971]

10. Harrison C, et al. JAK inhibition with ruxolitinib versus best available therapy for myelofibrosis. New England Journal of Medicine. 2012; 366:787–798. [PubMed: 22375970]

11. Tefferi A. JAK inhibitors for myeloproliferative neoplasms: clarifying facts from myths. Blood. 2012; 119:2721–2730. [PubMed: 22279053]

12. Tam CS, Verstovsek S. Investigational Janus kinase inhibitors. Expert Opinion on Investigational Drugs. 2013; 22:687–699. [PubMed: 23432430]

13. Harrison C, et al. Practical management of patients with myelofibrosis receiving ruxolitinib. Expert Review of Hematology. 2013; 6:511–523. [PubMed: 24083419]

14. Villeval JL, et al. High thrombopoietin production by hematopoietic cells induces a fatal myeloproliferative syndrome in mice. Blood. 1997; 90:4369–4383. [PubMed: 9373248]

15. Shivdasani RA, Fujiwara Y, McDevitt MA, Orkin SH. A lineage-selective knockout establishes the critical role of transcription factor GATA-1 in megakaryocyte growth and platelet development. EMBO J. 1997; 16:3965–3973. [PubMed: 9233806]

16. Vannucchi AM, et al. Development of myelofibrosis in mice genetically impaired for GATA-1 expression (GATA-1(low) mice). Blood. 2002; 100:1123–1132. [PubMed: 12149188]

17. Wen Q, et al. Identification of Regulators of Polyploidization Presents Therapeutic Targets for Treatment of AMKL. Cell. 2012; 150:575–589. [PubMed: 22863010]

18. Goldenson B, Crispino JD. The Aurora kinases in cell cycle and leukemia. Oncogene. 2014; 34:537–545. [PubMed: 24632603]

19. Levine RL, et al. Activating mutation in the tyrosine kinase JAK2 in polycythemia vera, essential thrombocythemia, and myeloid metaplasia with myelofibrosis. Cancer Cell. 2005; 7:387–397. [PubMed: 15837627]

20. Stachura DL, Chou ST, Weiss MJ. Early block to erythromegakaryocytic development conferred by loss of transcription factor GATA-1. Blood. 2006; 107:87–97. [PubMed: 16144799]

21. Vannucchi AM, et al. Abnormalities of GATA-1 in megakaryocytes from patients with idiopathic myelofibrosis. American Journal of Pathology. 2005; 167:849–858. [PubMed: 16127162]

22. Uozumi K, et al. Establishment and characterization of a new human megakaryoblastic cell line (SET-2) that spontaneously matures to megakaryocytes and produces platelet-like particles. Leukemia. 2000; 14:142–152. [PubMed: 10637490]

23. Mullally A, et al. Physiological Jak2V617F expression causes a lethal myeloproliferative neoplasm with differential effects on hematopoietic stem and progenitor cells. Cancer Cell. 2010; 17:584–596. [PubMed: 20541703]

24. Klampfl T, et al. Somatic mutations of calreticulin in myeloproliferative neoplasms. The New England Journal of Medicine. 2013; 369:2379–2390. [PubMed: 24325356]

25. Nangalia J, et al. Somatic CALR mutations in myeloproliferative neoplasms with nonmutated JAK2. The New England Journal of Medicine. 2013; 369:2391–2405. [PubMed: 24325359]

26. Goldenson B, Kirsammer G, Stankiewicz MJ, Wen QJ, Crispino JD. Aurora kinase A is required for hematopoiesis but is dispensable for mouse megakaryocyte endomitosis and differentiation. Blood. 2015; 125:2141–2150. [PubMed: 25670627]

27. den Hollander J, et al. Aurora kinases A and B are up-regulated by Myc and are essential for maintenance of the malignant state. Blood. 2010; 116:1498–1505. [PubMed: 20519624]

28. Wernig G, et al. The Jak2V617F oncogene associated with myeloproliferative diseases requires a functional FERM domain for transformation and for expression of the Myc and Pim proto-oncogenes. Blood. 2008; 111:3751–3759. [PubMed: 18216297]

29. Sumi K, Tago K, Kasahara T, Funakoshi-Tago M. Aurora kinase A critically contributes to the resistance to anti-cancer drug cisplatin in JAK2 V617F mutant-induced transformed cells. FEBS Letters. 2011; 585:1884–1890. [PubMed: 21557940]

30. Koppikar P, et al. Efficacy of the JAK2 inhibitor INCB16562 in a mouse model of MPLW515L–induced thrombocytosis and myelofibrosis. Blood. 2010; 115:2919–2927. [PubMed: 20154217]

31. Wernig G, et al. Efficacy of TG101348, a selective JAK2 inhibitor, in treatment of a mouse model of JAK2V617F–induced polycythemia vera. Cancer Cell. 2008; 13:311–320. [PubMed: 18394554]

32. Cowley DO, et al. Aurora-A kinase is essential for bipolar spindle formation and early development. Molecular & Cellular Biology. 2009; 29:1059–1071. [PubMed: 19075002]

33. Castro-Malaspina H. Pathogenesis of myelofibrosis: role of ineffective megakaryopoiesis and megakaryocyte components. Progress in Clinical & Biological Research. 1984; 154:427–454. [PubMed: 6089232]

34. Le Bousse-Kerdiles MC, Martyre MC, French IrnoIM. Involvement of the fibrogenic cytokines, TGF-beta and bFGF, in the pathogenesis of idiopathic myelofibrosis. Pathologie Biologie. 2001; 49:153–157. [PubMed: 11317961]

35. Martyre MC, Magdelenat H, Bryckaert MC, Laine-Bidron C, Calvo F. Increased intraplatelet levels of platelet-derived growth factor and transforming growth factor-beta in patients with myelofibrosis with myeloid metaplasia. British Journal of Haematology. 1991; 77:80–86. [PubMed: 1998600]

36. Bock O, et al. Bone morphogenetic proteins are overexpressed in the bone marrow of primary myelofibrosis and are apparently induced by fibrogenic cytokines. American Journal of Pathology. 2008; 172:951–960. [PubMed: 18349123]

37. Hoermann G, et al. Identification of oncostatin M as a JAK2 V617F–dependent amplifier of cytokine production and bone marrow remodeling in myeloproliferative neoplasms. FASEB Journal. 2012; 26:894–906. [PubMed: 22051730]

38. Chagraoui H, et al. Prominent role of TGF-beta 1 in thrombopoietin-induced myelofibrosis in mice. Blood. 2002; 100:3495–3503. [PubMed: 12393681]

39. Bruns I, et al. Megakaryocytes regulate hematopoietic stem cell quiescence through CXCL4 secretion. Nature Medicine. 2014; 20:1315–1320.

40. Zhao MPJ, Marshall H, Venkatraman A, Qian P, He XC, Ahamed J, Li L. Megakaryocytes maintain homeostatic quiescence and promote post-injury regeneration of hematopoietic stem cells. Nature Medicine. 2014; 20:1321–1326.

41. Schepers K, et al. Myeloproliferative neoplasia remodels the endosteal bone marrow niche into a self-reinforcing leukemic niche. Cell Stem Cell. 2013; 13:285–299. [PubMed: 23850243]

42. Dodson CA, Yeoh S, Haq T, Bayliss RA. kinetic test characterizes kinase intramolecular and intermolecular autophosphorylation mechanisms. Science Signaling [Electronic Resource]. 2013; 6 ra54.

References

43. Chou TC, Talalay P. Quantitative analysis of dose-effect relationships: the combined effects of multiple drugs or enzyme inhibitors. Advances in Enzyme Regulation. 1984; 22:27–55. [PubMed: 6382953]

44. Akashi K, Traver D, Miyamoto T, Weissman IL. A clonogenic common myeloid progenitor that gives rise to all myeloid lineages. Nature. 2000; 404:193–197. [PubMed: 10724173]
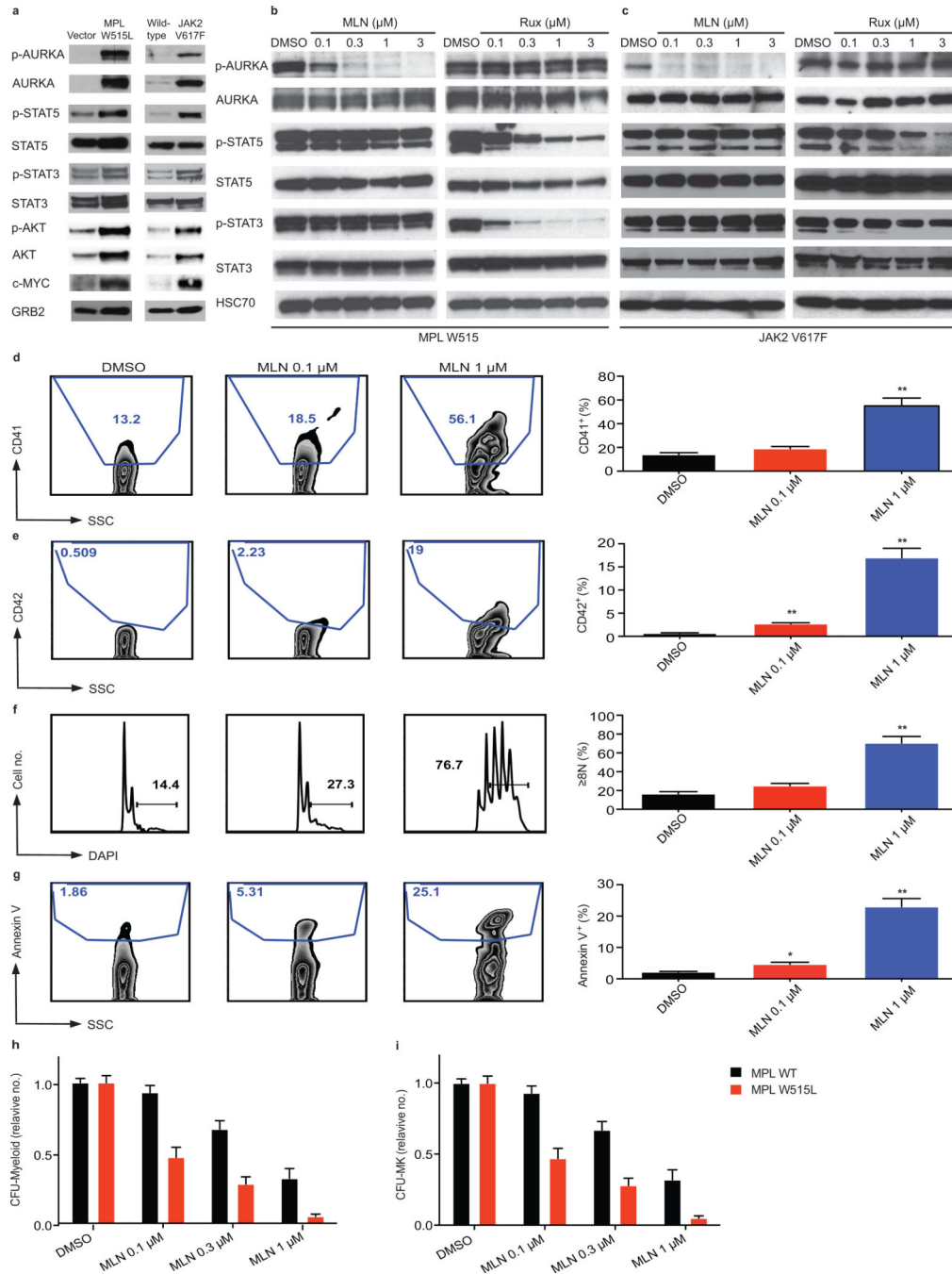
Figure 1. AURKA inhibition induces differentiation, polyploidization, apoptosis and proliferation arrest of primary mouse MPN cells

(**a**) Lysates from bone marrow cells of mice transplanted with the Migr1 vector or human MPLW515L or from wild-type or *Jak2^V617F* knock-in mice were probed for c-MYC and for activation of AURKA, STAT5, and AKT. GRB2 is shown as a loading control. (**b,c**) Cells from (**a**) were treated with DMSO, MLN8237 (MLN), or ruxolitinib (Rux) for 6 hours. Cell lysates were probed for activation of AURKA, STAT3, and STAT5. HSC70 is included as a loading control. (**d–g**) Mouse bone marrow lineage negative progenitor cells were
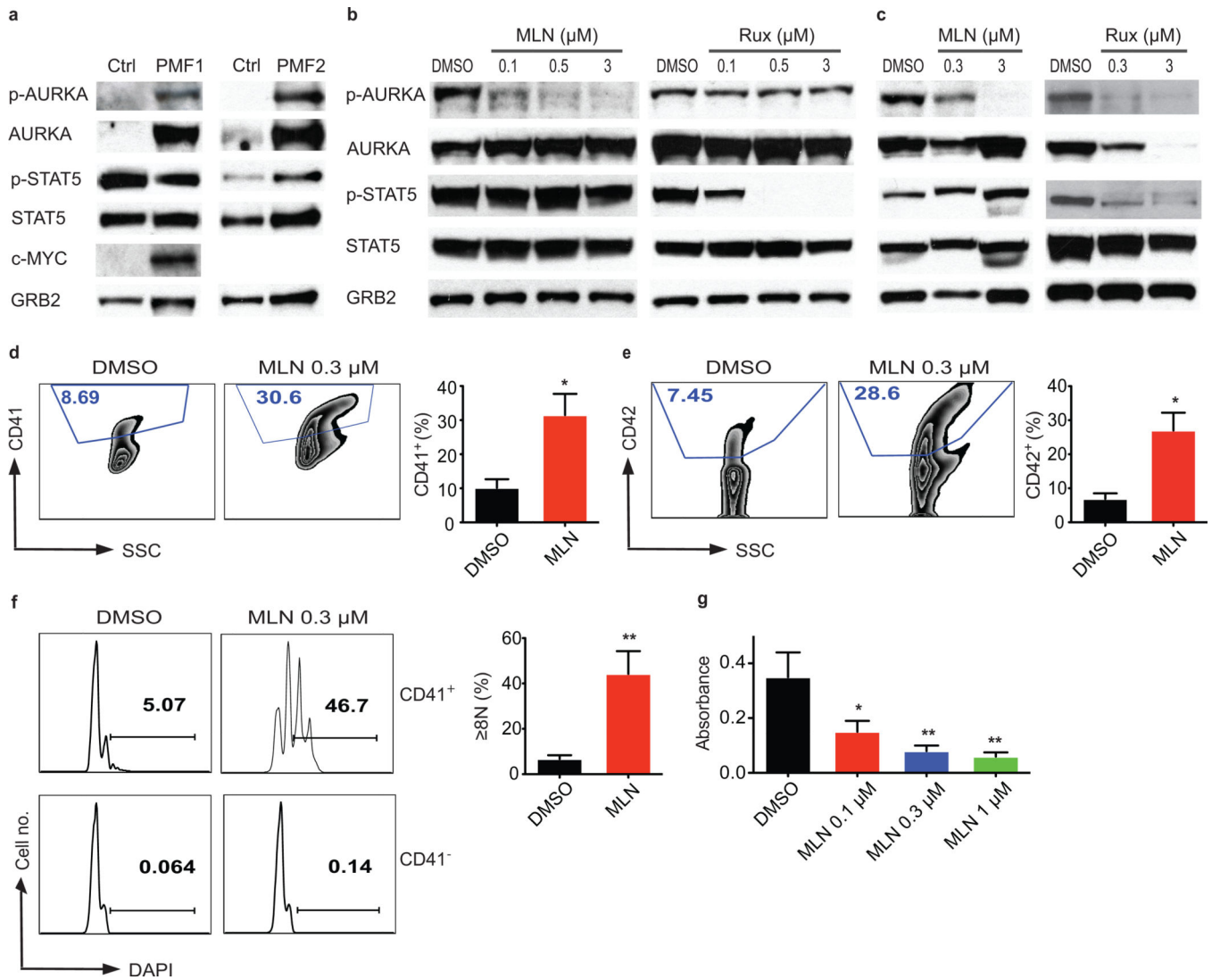
transduced with MPLW515L and cultured with DMSO or MLN8237 in the presence of THPO for 48 hrs. Flow cytometric determination of CD41 and CD42 (**d,e**), polyploidization (**f**), and apoptosis (**g**) of MPLW515L expressing bone marrow cells treated with DMSO or MLN. Shown are representative flow cytometry plots and bar graphs depicting the mean ± SD of two independent experiments conducted in triplicate; *p 0.05, **p 0.01, compared to DMSO by the unpaired two-sided Student's t test. (**h,i**) CFU-Myeloid and CFU-megakaryocyte (CFU-MK) of bone marrow cells from control bone marrow cells or those overexpressing MPLW515L. The number of colonies was normalized to DMSO treated cells. Bar graphs depict mean ± SD of two independent experiments conducted in duplicate. MPLW515L vs MPLWT, p 0.01 by two-way ANOVA (**h, i**).
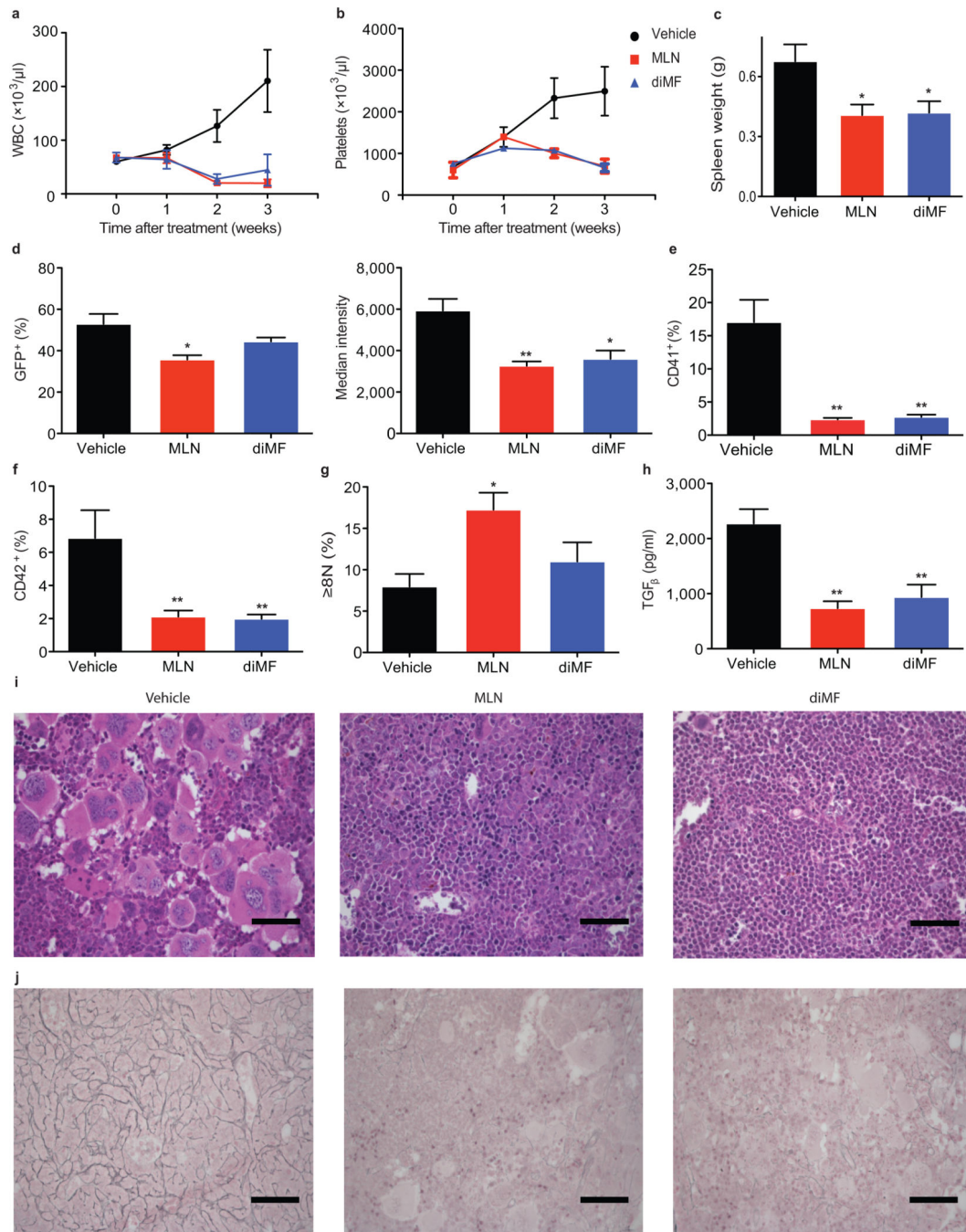
Figure 2. AURKA inhibition selectively induces polyploidization and differentiation of primary MPN patient samples

(**a**) Lysates from CD34^{+} cells of PMF patients were assayed for c-MYC, AURKA, and STAT signaling. Controls (Ctrl) are the cell lysates from CD34^{+} cells of human cord blood cells. (**b,c**) Western blots of lysates from CD34^{+} cells from patient PMF-3 were incubated with DMSO, MLN8237 or ruxolitinib for 6 hrs (**b**) or 48 hrs (**c**). (**d–g**), CD34^{+} cells from the peripheral blood of PMF patients (PMF-5 though 14) were cultured in the presence of DMSO or MLN8237 for 5 days in the presence of THPO. The expression of CD41 and CD42 (**d,e**), and DNA content (**f**) were determined by flow cytometry, and proliferation arrest of MPN cells as measured by Promega CellTiter proliferation assay (**g**). Results are representative of 10 specimens. For the flow cytometry data, representative plots (left) and bar graphs depicting mean ± SD (right) are shown. *p 0.05, **p 0.01, compared to DMSO by the unpaired two-sided Student's t test.

Figure 3. Inhibition of AURKA significantly reduces the disease burden in the MPLW515L mouse model of myelofibrosis

MPLW515L recipient mice were treated with 15mg/kg MLN8237 (MLN) or 60mg/kg diMF (diMF) for 3 weeks. (**a,b**) White cell (**a**) and platelet (**b**) counts following three weeks of treatment. MLN8237 vs vehicle and diMF vs vehicle, p 0.01 by two-way ANOVA. (**c**) Spleen weight of MLN8237, diMF and vehicle treated animals. (**d**) Percent of GFP+ cells and the degree of GFP intensity in the spleens of MPLW515L mice following treatment with MLN8237, diMF or vehicle. (**e,f**) The percentage of CD41$^+$ (**e**), and CD42$^+$ (**f**), cells in the

bone marrow of treated animals. (**g**) DNA content of megakaryocytes stained with CD41 and DAPI. (**h**) TGF-β levels in the plasma of MLN8237, diMF and vehicle treated mice. (**i,j**) H&E (**i**) and reticulin (**j**) stained sections of bone marrow from MLN8237, diMF and vehicle treated animals. Scale bars depict 50 microns. Results are representative of 2 independent experiments. n=6 animals per group. Bar graphs and line graphs depict mean ± SD. *p 0.05, **p 0.01, compared to vehicle determined by the unpaired two-sided Student's t test.
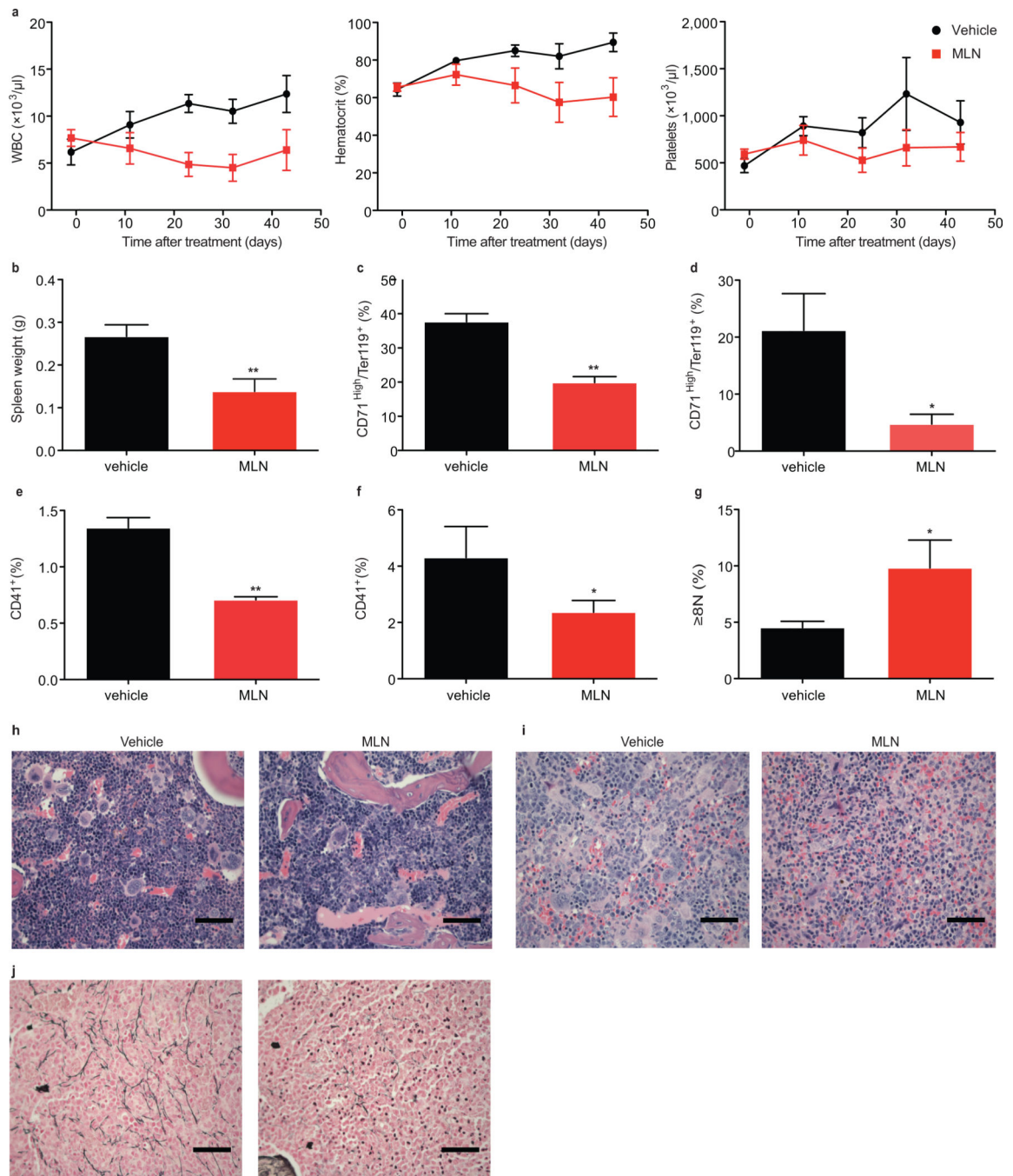
Figure 4. MLN8237 reduced the disease burden of JAK2V617F induced MPN in vivo

Transplant recipients of *Jak2*[V617F] bone marrow cells were treated with 15 mg/kg MLN8237 for 7 weeks. (**a**) White blood cell count, hematocrit and platelet count in the peripheral blood of MLN8237 and vehicle treated animals. MLN8237 vs vehicle, p 0.01 (**a, b**); MLN vs vehicle, p 0.05 (**c**), by two-way ANOVA. (**b**) Spleen weights of MLN837 versus vehicle treated mice. (**c–g**) Flow cytometry measurements of bone marrow and spleen CD71^{high}/Ter119^{+} erythroid cells (**c,d**), megakaryocytes (**e,f**) and the ploidy state of CD41^{+} bone marrow megakaryocytes (**g**). (**h,i**) H&E stained sections of bone marrow (**h**) and spleen (**i**).

(**j**) Reticulin staining of bone marrow sections. Scale bars depict 50 microns. Results are representative of 2 experiments. n=7 animals per group. Line graphs and bar graphs depict mean ± SD. *p 0.05, **p 0.01, compared to vehicle by the unpaired two-sided Student's t test.
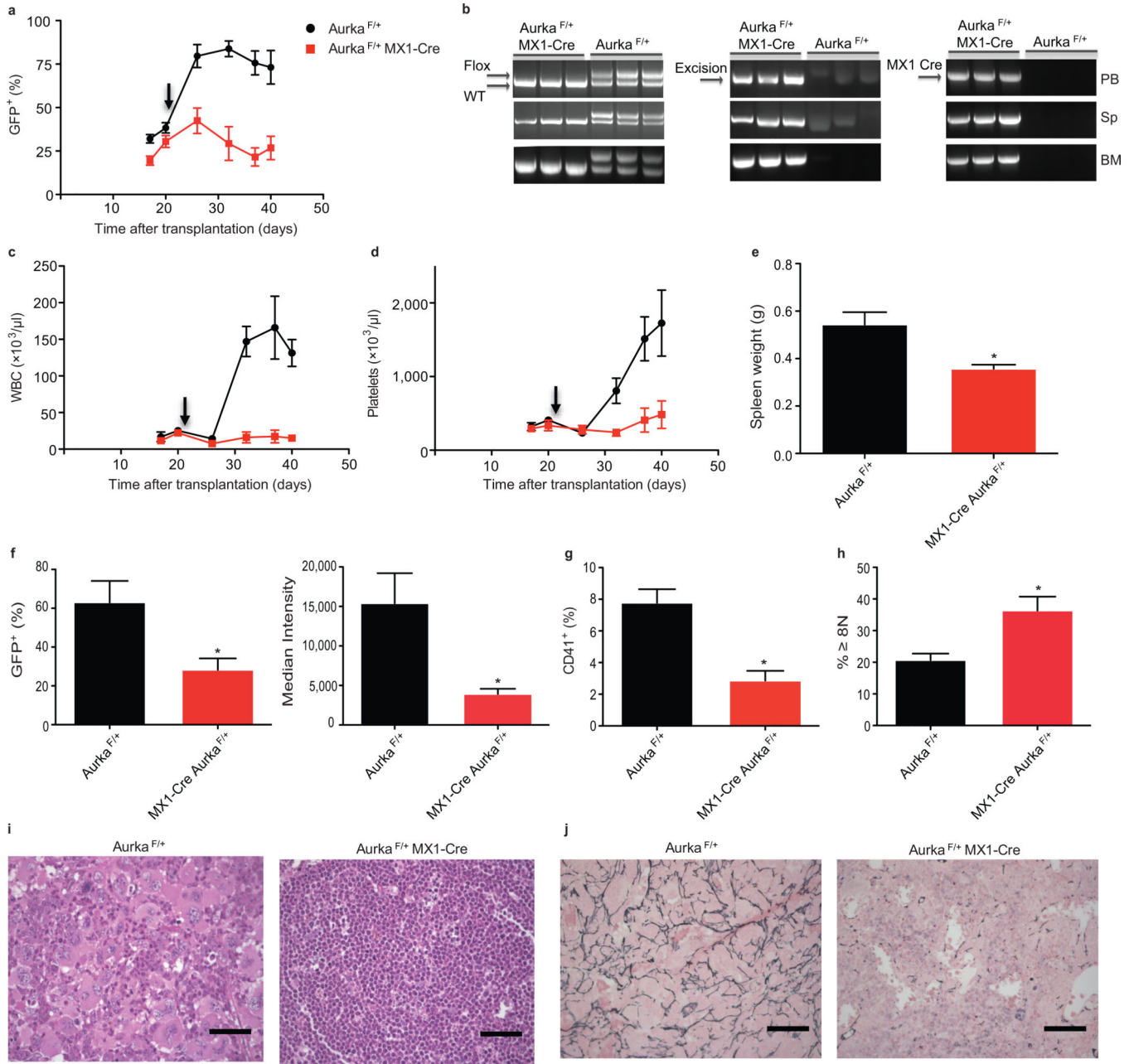
Figure 5. Heterozygous deletion of *Aurka* is sufficient to reduce the disease burden in the MPLW515L mouse model of myelofibrosis

Bone marrows from *Aurka*[F/+] or *Aurka*[F/+] MX1-Cre mice were transduced with MPLW515L and transplanted into recipient animals. pI-pC was injected into recipients three weeks after transplant to induce excision of *Aurka* by MX-1Cre (arrows in **a,c,d**). (**a**) Percentage of GFP+ cells in the peripheral blood of mice following pIpC administration. (**b**) PCR determination of deletion of the floxed region, excision products and MX1-Cre expression in the peripheral blood (PB), spleen (Sp) and bone marrow (BM) of recipient mice 19 days after the first injection of pI-pC. (**c,d**) White blood (**c**) and platelet (**d**) counts of *Aurka*[F/+] vs *Aurka*[F/+] MX1-Cre mice following the deletion of one allele of Aurka.

Aurka$^{F/+}$ vs *Aurka*$^{F/+}$ MX1-Cre, p 0.01 by two-way ANOVA (**a,c,d**). (**e**) Spleen weight of *Aurka*$^{F/+}$ vs *Aurka*$^{F/+}$ MX1-Cre mice post pIpC treatment. (**f–h**) Flow cytometry measurement of GFP$^+$ tumor burden (**f**), CD41$^+$ megakaryocytes (**g**), and DNA content of the megakaryocytes in the spleen (**h**). (**i**) H&E stained sections of the bone marrow. (**j**) Reticulin staining of the bone marrow. Scale bars depict 50 microns. Results are representative of 2 independent experiments. n=5 animals per group. Bar graphs and line graphs depict mean ± SD. *p 0.05, **p 0.01, compared to *Aurka*$^{F/+}$ mice by the unpaired two-sided Student's t test.
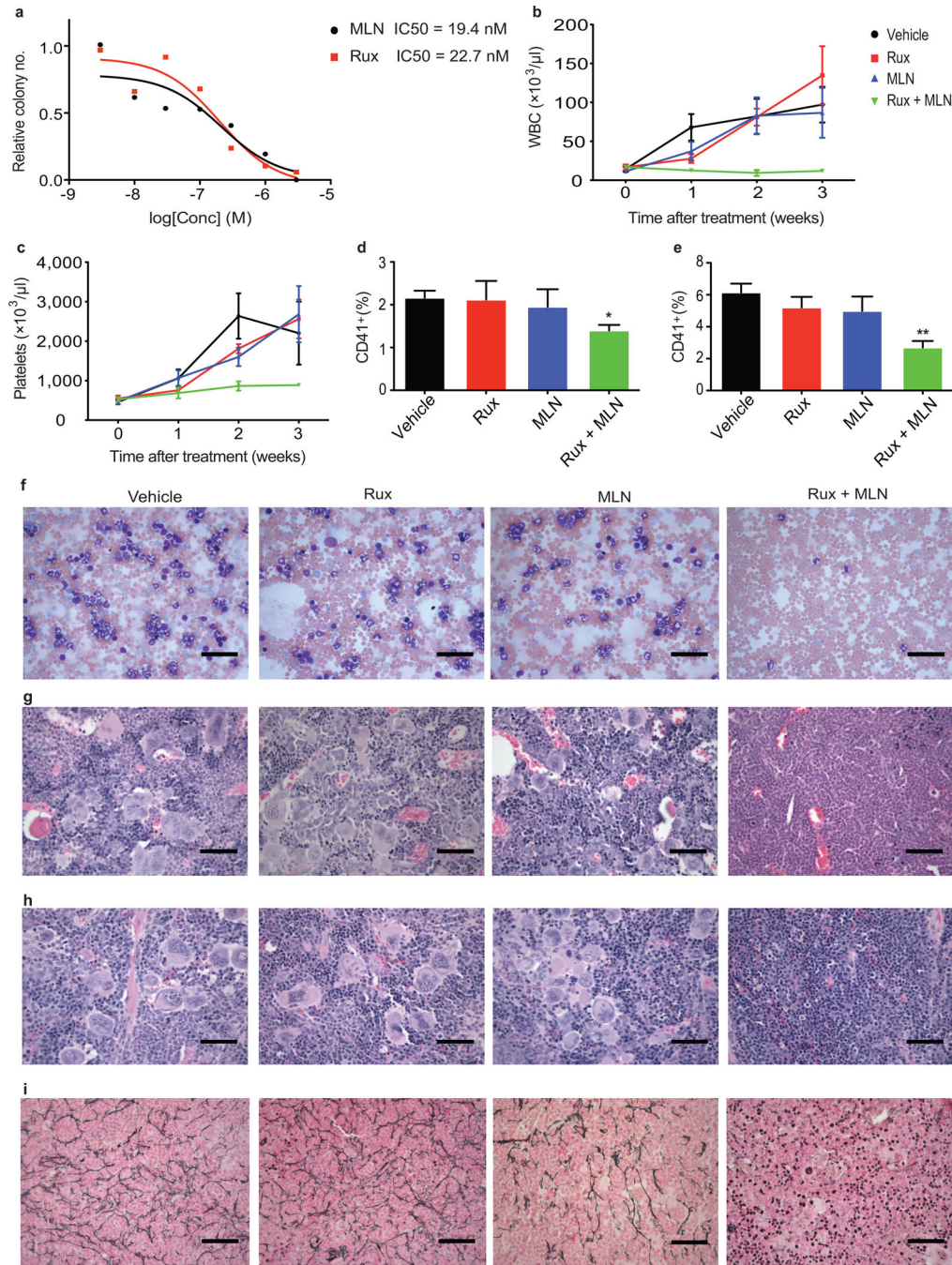
Figure 6. MLN8237 and ruxolitinib act synergistically both in vitro and in vivo
(**a**) Determination of IC50 values of MLN8237 (MLN) and ruxolitinib (Rux) derived from treatment of myeloid colony formation with increasing doses of the drugs. (**b,c**) White blood cell (**b**) and platelet counts (**c**) of MPLW515L mice treated with sub-maximal doses of MLN8237 or ruxolitinib, or their combination. MLN8237 + Rux vs vehicle, p   0.01, while Rux vs vehicle, MLN8237 vs vehicle, P   0.05, by two-way ANOVA. (**d**) Measurement of CD41^{+} megakaryocytes in the bone marrow (**e**) and spleen (**f**) of treated animals. (**f–h**) May-Grunwald Giemsa stained blood smears (**f**) and H&E stained sections of the bone marrow

(**g**), and spleen (**h**) of treated mice. (**i**) Reticulin staining of bone marrow sections of treated mice. Scale bars depict 50 microns. Results are representative of 2 independent experiments. n=5 animals per group. Bar graphs and line graphs depict mean ± SD. *p 0.05, **p 0.01, compared to vehicle by the unpaired two-sided Student's t test.